CONCLUSION

Our comparison of experimental data with theoretical results shows qualitative agreement; and at low concentrations, also quantitative. But there are a number of facts that cannot be explained in the model based on an Ising type of magnetic ordering of the Ho^{3+} ions in the garnet structure. This, for example, the experimental critical points are all of the same order of magnitude, whereas in the theory the critical point for $\mathbf{H}\parallel\langle 001\rangle$ lies lower than for the other magnetic-field directions. The critical temperatures given by the Ising model in the case of field directions $\langle 111\rangle$ and $\langle 110\rangle$ are higher than the experimental. Thus although for concentration $x=0.67$ the numerical results for the proposed model are close to the experimental, for concentration $x=1.05$ the disagreement between theory and experiment for T_{cr} (in the case of these field directions) is ~7 K. This is especially noticeable for the loop in Fig. 2c.

The deviations from experiment can be explained as follows. We carried out the analysis of the phase diagrams by considering only the ground quasi-doublet of the Ho^{3+} ions in the crystalline field, neglecting the influence of the higher-placed levels. Allowance for higher-lying levels will lead to a faster decrease of the moment of the RE sublattices with increase of temperature, and consequently to a lowering of T_{cr}. Furthermore, as was mentioned earlier,[1] when $x>x_c$ the external field is parallel to the exchange field and causes one of the components of the quasidoublet to draw nearer to the higher-lying levels, and with increase of temperature the sharpest deviation from the theoretical model should therefore be observed precisely in the upper right part of the H-T diagram. Both of these factors leads to the result that compensation of the moments of the RE and iron sublattices sets in at a lower T as compared with the model.

As calculations show, the presence of a gap of order 5 cm^{-1} (such a value for the energy of the gap follows from data of other authors[5]) has practically no effect on the quantitative calculations for $x\leq 0.1$. Therefore the model uses only the following parameters: H_{mol}, μ_R and $\mathbf{M}_{Fe}$. Qualitative agreement with experiment is then observed up to concentration $x=1.25$. In fact, the behavior of the experimental lines of phase transitions on the H-T-x diagrams corresponds to the behavior of the calculated lines of phase transitions given by this simple model.

[1] V. I. Silant'ev, A. I. Popov, R. Z. Levitin, and A. K. Zvezdin, Zh. Eksp. Teor. Fiz. 78, 640 (1980) [Sov. Phys. JETP **51**, 323 (1980)].

[2] V. G. Demidov, Author's abstract of candidate's dissertation, Moscow State University, 1977.

[3] R. Z. Levitin and Yu. F. Popov, in: Ferrimagnetizm (Ferrimagnetism), Moscow State University, 1975, p. 6.

[4] J. S. Griffith, Phys. Rev. 132, 316 (1963).

[5] V. Nekvasil, Phys. Status Solidi (b) **94**, K41 (1979); P. Novák, V. Nekvasil, T. Egami, P. J. Flanders, E. M. Gyorgy, and L. G. Van Uitert, Abstracts of Conference of CMEA (Council for Mutual Economic Assistance, Sovet ékonomicheskoĭ vzaimopomoshchi, SEV) Countries on Physics of Magnetic Materials, Jaszowiec, Poland, 1980, p. I–17; P. Nóvak, V. Nekvasil, T. Egami, P. J. Flanders, E. M. Gyorgy, L. G. Van Uitert, and W. H. Grodkiewicz, J. Magnetism and Magnetic Materials 22, 35 (1980).

[6] R. Alben, Phys. Rev. B2, 2767 (1970).

[7] L. D. Landau and E. M. Lifshitz, Statisticheskaya fizika (Statistical Physics), 3d ed., M.: Nauka, 1976, Part 1, p. 486 (transl., Pergamon Press, 1980).

Translated by W. F. Brown Jr.

Investigation of the structure of some smectic *A*, *B*, and *E* phases

L. I. Mineev, L. A. Val'kova, L. S. Shabyshev, and I. G. Chistyakov

Ivanovo State University

(Submitted 8 September 1980)
Zh. Éksp. Teor. Fiz. **80**, 1963–1968 (May 1981)

The structures of the smectic *A*, *B*, and *E* phases of butyl *p*-phenylbenzal-*p'*-aminocinnamate (BPBAC) oriented by a magnetic field are investigated by x-ray diffraction and microscopic analysis. It is observed that the ordering of the molecular structure of the *E* phase is higher than that of the high-temperature *A* and *B* phases. An attempt is made to describe the smectic *E* phase by means of a three-dimensional rhombic lattice structure. The optical analogy method is employed to verify the concepts regarding the structure of the smectic phases. On the basis of this investigation one can ascribe to the *A*, *B*, and *E* phases, symmetry symbols derived from the statistical distribution functions namely $C(B)$: 2, $a/2$; $C(A_2)$: 2, $a/2$, and $C(A_i)$: 2, $b/2$ respectively.

PACS numbers: 61.30.Eb, 61.30.Gd

The goal of our work was to study the smectic structure of the fourth homolog in the *n*-alkyl *p*-phenylbenzal-*p'*-aminocinnamate (BPBAC) series. $C_6H_5-C_6H_4-CH-N-C_6H_4-CH-CH-CO\cdot OC_4H_9$, which has a smectic *E* phase in addition to *A* and *B* mesophases. The synthesis and identification of the mesophases of this ma-

FIG. 1. Conoscopic figure of the smectic E phase of BPBAC for a diagonal position of the sample relative to the plane of polarization.

terial has been described previously.[1]

The relatively high order of the E mesophase makes its structural study especially interesting. Results of the investigation of the properties of this mesomorphic state are given in a number of papers,[2-5] but structural investigations have still clearly been inadequate.

The scheme for BPBAC phase transitions is the following:

$$\text{Solid crystal} \xleftrightarrow{77\,^\circ\mathrm{C}} C_E \xleftrightarrow{107\,^\circ\mathrm{C}} C_B \xleftrightarrow{172\,^\circ\mathrm{C}} C_A \xleftrightarrow{208^\circ\mathrm{C}} \text{Isotropic liquid}$$

The x-ray diffraction analysis was performed using photographic recording of the diffraction pattern. CuK_α radiation was used with monochromatization by a nickel filter. A thermostatted cell with the test material was placed in a magnetic field of $B = 15,000$ G, which was used to orient the sample. Orthoscopic and conoscopic studies were performed with a MIN-8 polarizing microscope.

Conoscopic studies indicate that the A and B phases are optically positive and uniaxial. This means that there is no matched molecular tilt in the smectic layers. In the smectic E phase, BPBAC is optically biaxial and positive, as is seen from the conoscopic figure given on Fig. 1 and is in agreement with literature data.[5] The biaxiality of the E phase allows us to assign this phase according to one of three syngonies: triclinic, monoclinic, or rhombic. From measurement of the conoscopic angles[6] we calculated the biaxiality angle as 32± 2°.

The x-ray diffraction pattern obtained from the BPBAC sample oriented by a magnetic field in the A, B, and E phases are shown on Fig. 2, where the hkl indices of the reflections on each layer $00l$ are indicated. On Fig. 3a we give the x-ray diffraction pattern of the smectic E phase of BPBAC. The calculated and measured interplanar separations corresponding to this phase are given in Table I.

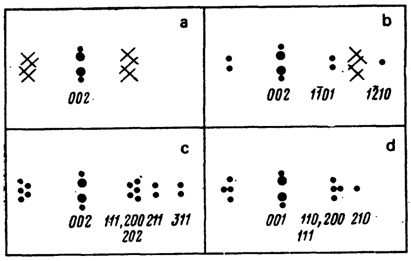

FIG. 2. X-ray diffraction patterns for the phases (a) A, (b) B, (c, d) E of BPBAC.

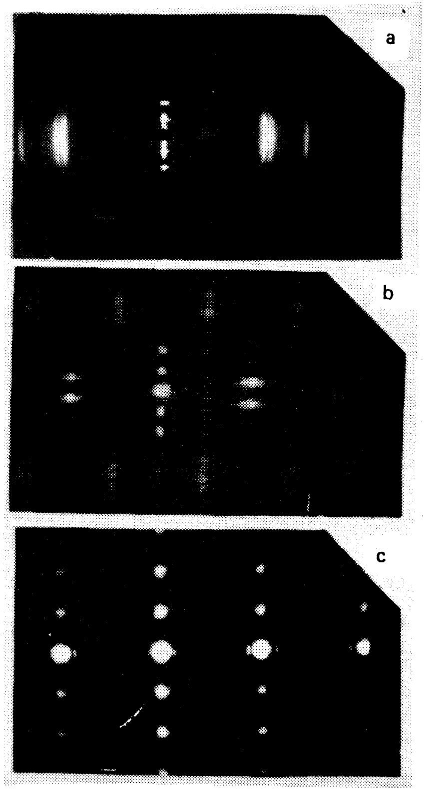

FIG. 3. X-ray diffraction patterns of (a) the E phase, (b) its two-dimensional optical analog, and (c) the optical diffraction pattern modeling the equatorial reflection of the x-ray diffraction pattern of the supercooled E phase of BPBAC.

The presence of a diffuse equatorial reflection on the diffraction pattern of the high-temperature smectic modification makes it possible to identify it as an A phase (Fig. 2a).

In the smectic B phase (Fig. 2b) the equatorial reflection becomes more pronounced; this suggests that the molecular order within the layers is higher than in the smectic A phase. The distribution pattern for the centers of gravity of the molecules in the projection on the plane parallel to the axis of the texture is also evidence for this; we obtained this pattern by optical synthesis from models of the diffraction patterns of smectic A and B states (Fig. 4) using a method given in Ref. 7. On the figure it is seen that the interaction radius in phase A is significantly smaller than in B (both in the

TABLE I.

hkl	Interplanar separations		Intensity
	d_{meas}	d_{calc}	
0 0 2	26,20	26.20	Strong
1 1 1	4.31	4,31	Strong
2 0 0	4.00	4.00	Very strong
2 1 1	3.16	3,15	Weak
3 1 1	2,38	2.37	Very weak

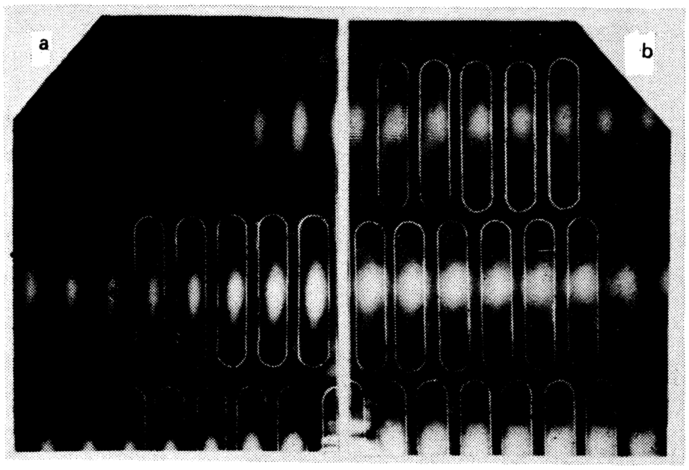

FIG. 4. Distribution pattern for the centers of gravity of molecules in a projection on the plane parallel to the texture axis, for the smectic (a) *A* and (b) *B* phases of BPBAC.

layer and lateral packing of the molecules). We note that in the *B* phase new reflections appear: $1\bar{1}01$ and $1\bar{2}10$.

At a temperature of 107 °C, at large angles we see on the diffraction pattern (Figs. 2c and 3a) the reflections 111, 200, 202, 211, and 311 due to two-dimensional molecular order within the layer. The corresponding diffraction angles are 10.3, 11.1, 14.1, and 18.9°. This gives us a basis for classifying the low-temperature phase of BPBAC as the *E* modification.[2] When the *E* phase is supercooled below the melting point, new reflections are noted on the diffraction pattern obtained for a sample temperature of 50 °C: 110 and 210 (Fig. 2d).

The identification of reflections, and also the biaxiality and centrosymmetry of the conoscopic figure, make it possible to assign the structure of the *E* phase of BPBAC to the rhombic system. The extinction condition for the reflections ($k+l$ with odd values are extinguished) makes it possible to identify the lattice type of the non-supercooled *E* phase as base-centered *A*. The principle of closest packing requires the presence of not one, but two molecules at each lattice point of the selected cell. In adjacent layers, the molecules are arranged so that pairs of molecules of the upper plane are located over the intervals between molecules of the lower layer; i.e., their symmetry transformation by a glide reflection plane is possible. However, such a structural molecular pattern presupposes as *F* face-centered lattice; then one molecule would be located at each point of this lattice. For an *F* face-centered lattice, only those reflections should be present for which $h+k$, $k+l$, and $h+l$ are even. This condition is not satisfied, since the 211 reflections are present. It is reasonable to assume that the *A* base-centered lattice is correctly chosen, since if we assume that the pairs of molecules at the lattice points have antiparallel packing, then the transition to an *F* face-centered cell becomes impossible. The hypothesized structural pattern formed from pairwise interacting molecules with an antiparallel arrangement is illustrated in Fig. 5. In accordance with the classification proposed in Ref. 8, the symmetry symbol of the *E* phase has the form

$$C(A_i):2,\ b/2,$$

where *A* means that the perturbation of the lattice pattern is characterized by a first-order distribution function $W_1(x, y)$; *i* indicates the type of lattice; 2 designates a two-fold axis connected with the antiparallel arrangement of the molecules in the layer, $b/2$ indicates the presence of a glide reflection plane with translation $b/2$. In accordance with the assumed notation for the symmetry space groups, we may ascribe the international symbol for the space group to the index *i*.[9] This designation will be completely valid for the immediate environment of the molecules. The relative paucity of reflections on the x-ray diffraction pattern of the liquid-crystal state prevent us from unambiguously determining the space group. Therefore to describe the smectic phases we use symmetry symbols containing statistical distribution functions obtained directly from the x-ray diffraction experiment and reflecting the disorder of the liquid-crystal state.

The smectic *E* phase is the most ordered, but the fact that on the diffraction pattern there are simultaneously reflections with indices of the type 11*l*, 20*l*, 21*l* suggests that the sample is cylindrically symmetric. Rotation of the sample about the texture axis does not lead to extinction of the reflections due to the intralayer periodicity, as would have been the case for a liquid-crystal monodomain.

If the molecules of the upper layer are arranged above the molecules of the lower layer, then certain reflections may occur which would make up an equatorial reflection. In order to confirm this, we present on Fig. 3c the diffraction pattern from a two-dimensional model having such a molecular packing. The

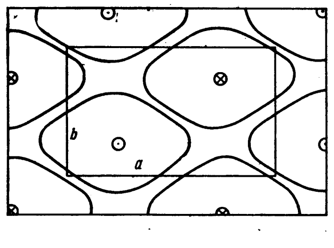

FIG. 5. Packing diagram for BPBAC molecules in the plane of the smectic layer of the *E* phase. $a = 8$ Å, $b = 5.1$ Å, $c = 52.4$ Å.

reason for the reflections is easily explained if we assign the indices *hkl* to them. For the meridian direction the reflections are identified as 001, 002, . . . ; for the equatorial direction, 001, 020, . . . , 011, 012, . . . , 021, 022, ... Such an intensity distribution is observed on the diffraction pattern from the supercooled *E* phase of BPBAC (Fig. 2d). The lattice in this case is primitive. We must point out that the shown optical diffraction pattern explains the form of only the equatorial reflections 110 and 111, since only a two-dimensional cross section is modeled.

An interesting characteristic of this compound is its high degree of order. Along the meridian of the x-ray diffraction pattern we observe up to five orders of reflections. The diffusional maxima on the layer lines exhibit intramolecular interference, which is usually blurred by the background. Analysis of the intramolecular scattering shows that beginning with the fourth meridional reflection, a diffuse background appears along the layer reflections, and the directions of maximum intensity from a cross (Fig. 3a). Such a situation may arise when screw axes are present in the molecular structure. This is indeed possible, since it is known that in biphenyl and in Schiff's bases, the phenyl rings are out of alignment by 42° (Ref. 10) and 50° (Ref. 11) respectively. On Fig. 3b we display the optical diffraction pattern from the model, confirming the presence of a screw axis in the molecules or a glide reflection plane; these do not cause the sample as a whole to have optical activity, just as optically-active chiral smectics do not exhibit specific singularities in the diffraction experiment.

The transition to the smectic *B* phase is accompanied by a change of the rhombic lattice to a hexagonal one, and the correlation of molecules along the director is retained. The x-ray diffraction pattern of the smectic *B* phase of BPBAC (Fig. 2b) indicates extinction of reflections of odd order on the zero-layer pattern. A $1\bar{1}01$ reflection appears at the location of the 111 and 200 reflections together with a very weakly visible $1\bar{2}10$ reflection. The interplanar separations are respectively $d(1\bar{1}01)=4.29$ Å and $d(1\bar{2}10)=2.47$ Å. These values are in good agreement with hexagonal packing of molecules for $a=(2/\sqrt{3})$ and $d(1\bar{1}01)=2d(1\bar{2}10)=4.95$ Å. The 211 reflection on the x-ray diffraction pattern is shifted to lower angles with considerable blurring, and the $2\bar{2}01$ reflection (obligatory for hexagonal packing) is not observed in this case. We explain this by the fact that in the *B* phase there is also pairwise interaction of molecules, although the translational long-range order of these pairs is disrupted. They become isolated from one another, and the statistical thermal motion of the molecules has a cooperative character. The diffraction pattern, as well as the fact that the conoscopic figure of the *B* phase is uniaxial, allows us to assign to the structure the symmetry symbol $C(A_2):2, a/2$, where $i=2$ means that the lattice is hexagonal in this case. Apparently, the absence of a diffuse reflection on the x-ray diffraction patterns from the *B* phase may be a consequence of the absence both of pairwise interaction and of cooperative random motion. Analogous hypotheses have been expressed previously,[12] but proper attention has not been paid to this reflection. The angular position of this diffraction maximum corresponds to 3.65 Å, i.e., to the smallest separation between interacting molecules in the pair. This value is obtained taking into account the coefficient 1.117 from the Bragg formula. The necessity for introducing the de Vries coefficient is due to the very nature of x-ray scattering from an isolated, randomly rotating pair of molecules.[13]

Transition from the smectic *B* to the *A* phase leads to blurring of the $1\bar{1}01$ reflection into a diffuse spot, which characterizes a random distribution of centers of gravity of the molecules in the plane of the layer; taking into account the uniaxiality of the conoscopic figure, this allows us to ascribe to the *A* phase the symmetry symbol $C(B):2, a/2$, where *B* means that the lattice disturbances are characterized by a second-order distribution function $W_2(x, y)$.

[1] A. M. Shabysheva, L. S. Shabyshev, L. A. Val'kova, and L. N. Zhukova, in: Zhidkie Kristally (Liquid Crystals), Izdat. IvGU, Ivanovo, 1981.

[2] S. Diele, P. Brand, and H. Sackmann, Mol. Cryst. Liq. Cryst. 17, 163 (1972).

[3] S. Diele, Phys. Status Solidi A 25, K183 (1974).

[4] J. Doucet, A. Levelut, and M. Zimbert Lambert, J. Phys. (Paris) 36, 1 (1975).

[5] J. W. Goodby and G. W. Gray, Mol. Cryst. Liq. Cryst. 49, 165 (1979).

[6] L. I. Mineev and I. G. Chistyakov, in: Zhidkie Kristally (Liquid Crystals), Izdat. IvGU, Ivanovo, 1977, p. 7.

[7] B. K. Vaĭnshtein, I. G. Chistyakov, E. A. Kosterin, V. M. Chaĭkovskiĭ, and A. D. Inozemtseva, Kristallografiya 16, 717 (1971) [Sov. Phys. Crystallogr. 16, 624 (1971)].

[8] B. K. Vainshtein and I. G. Chistyakov, Acta Cryst. A28, 134 (1972) [sic].

[9] A. de Vries, J. Chem. Phys. 70, 2705 (1979).

[10] G. B. Bokiĭ, Kristallokhimiya, (Crystal Chemistry), 3rd. Ed. Nauka, Moscow, 1971, p. 371.

[11] V. M. Potapov, Stereokhimiya (Stereochemistry), Khimiya, Moscow, 1976, p. 569.

[12] A. I. Aleksandrov, Cand. Dissert, Moscow, 1977.

[13] A. de Vries, Mol. Cryst. Liq. Cryst. 10, 219 (1970); 11, 361 (1970).

Translated by Cathy Flick